Ocean acidification impacts growth and shell mineralization in juvenile abalone (Haliotis tuberculata)

Stéphanie Auzoux-Bordenave, Nathalie Wessel, Aïcha Badou, Sophie Martin, Saloua M'Zoudi, Solène Avignon, Sabine Roussel, Sylvain Huchette, Philippe Dubois

Marine Biology

Ocean acidification impacts growth and shell mineralization in juvenile abalone (Haliotis tuberculata)

--Manuscript Draft--

Manuscript Number:	MABI-D-19-00091R4
Full Title:	Ocean acidification impacts growth and shell mineralization in juvenile abalone (Haliotis tuberculata)
Article Type:	Original paper
Keywords:	ocean acidification; abalone; juvenile; growth; shell mineralization
Corresponding Author:	Stephanie Auzoux-Bordenave, PhD Sorbonne Universite Concarneau, FRANCE
Corresponding Author Secondary Information:	
Corresponding Author's Institution:	Sorbonne Universite
Corresponding Author's Secondary Institution:	
First Author:	Stephanie Auzoux-Bordenave, PhD
First Author Secondary Information:	
Order of Authors:	Stephanie Auzoux-Bordenave, PhD
	Nathalie Wessel
	Aïcha Badou
	Sophie Martin
	Saloua M'Zoudi
	Solène Avignon
	Sabine Roussel
	Sylvain Huchette
	Philippe Dubois
Order of Authors Secondary Information:	
Funding Information:	Ministère de l'Enseignement Supérieur et de la Recherche, Paris, FR — Dr Nathalie Wessel Ministère de l'Enseignement Supérieur et de la Recherche, Paris, FR — Dr Stephanie Auzoux-Bordenave Fondation pour la Recherche sur la Biodiversité (FRB) (FR) — Dr Stephanie Auzoux-Bordenave
Abstract:	Ocean acidification is a major global driver that leads to substantial changes in seawater carbonate chemistry, with potentially serious consequences for calcifying organisms. Marine shelled molluscs are ecologically and economically important species, providing essential ecosystem services and food sources for other species. Due to their physiological characteristics and their use of calcium carbonate (CaCO3) to build their shells, molluscs are among the most vulnerable invertebrates with regard to ocean acidification, with early developmental stages being particularly sensitive to pH changes. This study investigated the effects of CO2-induced ocean acidification on juveniles of the European abalone Haliotis tuberculata, a commercially important gastropod species. Six-month-old juvenile abalones were cultured for 3 months at four pH levels (8.1, 7.8, 7.7, 7.6) representing current and predicted near-future conditions. Survival, growth, shell microstructure, thickness and strength were compared across the four pH treatments. After three months of exposure, significant reductions in

	juvenile shell length, weight and strength were revealed in the pH 7.6 treatment. SEM observations also revealed modified texture and porosity of the shell mineral layers as well as alterations of the periostracum at pH 7.6 which was the only treatment with an aragonite saturation state below 1. It is concluded that low pH induces both general effects on growth mechanisms and corrosion of deposited shell in H. tuberculata. This will impact both the ecological role of this species and the costs of its aquaculture.

Ocean acidification impacts growth and shell mineralization in juvenile abalone (*Haliotis tuberculata*)

Stéphanie Auzoux-Bordenave[1,8*], Nathalie Wessel[2], Aïcha Badou[3], Sophie Martin[4,8], Saloua M'Zoudi[5], Solène Avignon[1], Sabine Roussel[6], Sylvain Huchette[7], Philippe Dubois[5]

[1]UMR "Biologie des Organismes et Ecosystèmes Aquatiques" (BOREA), /MNHN/CNRS/ SU/IRD/, Muséum National d'Histoire Naturelle, Station Marine de Concarneau, 29900 Concarneau, France
[2]Ifremer, Département Océanographie et Dynamique des Ecosystèmes (ODE), Rue de l'île d'Yeu, BP21105, 44311 Nantes Cedex 3, France
[3]Muséum National d'Histoire Naturelle, Station Marine de Concarneau, 29900 Concarneau, France
[4]UMR 7144 "Adaptation et Diversité en Milieu Marin" (AD2M), CNRS/SU, Station Biologique de Roscoff, 29680 Roscoff Cedex, France
[5]Laboratoire de Biologie Marine, Université Libre de Bruxelles, CP160/15, 1050, Brussels, Belgium
[6]Univ Brest, CNRS, IRD, Ifremer, LEMAR, 29280 Plouzané, France
[7]Ecloserie France Haliotis, Kerazan, 29880 Plouguerneau, France
[8]Sorbonne Université (SU), 4, place Jussieu, 75005 Paris, France

* Corresponding author: tel: + 33 2 98 50 42 88; fax: + 33 2 98 97 81 24,
E-mail: stephanie.auzoux-bordenave@mnhn.fr

Abstract

Ocean acidification is a major global driver that leads to substantial changes in seawater carbonate chemistry, with potentially serious consequences for calcifying organisms. Marine shelled molluscs are ecologically and economically important species, providing essential ecosystem services and food sources for other species. Due to their physiological characteristics and their use of calcium carbonate ($CaCO_3$) to build their shells, molluscs are among the most vulnerable invertebrates with regard to ocean acidification, with early developmental stages being particularly sensitive to pH changes. This study investigated the effects of CO_2-induced ocean acidification on juveniles of the European abalone *Haliotis tuberculata*, a commercially important gastropod species. Six-month-old juvenile abalones were cultured for 3 months at four pH levels (8.1, 7.8, 7.7, 7.6) representing current and predicted near-future conditions. Survival, growth, shell microstructure, thickness and strength were compared across the four pH treatments. After three months of exposure, significant reductions in juvenile shell length, weight and strength were revealed in the pH 7.6

treatment. SEM observations also revealed modified texture and porosity of the shell mineral layers as well as alterations of the periostracum at pH 7.6 which was the only treatment with an aragonite saturation state below 1. It is concluded that low pH induces both general effects on growth mechanisms and corrosion of deposited shell in *H. tuberculata*. This will impact both the ecological role of this species and the costs of its aquaculture.

Keywords: ocean acidification; abalone; juvenile; growth; shell mineralization

Introduction

Anthropogenic carbon dioxide emission and its subsequent absorption by the ocean is responsible for seawater pH decrease and reduced availability of carbonate ions, leading to a decrease of calcium carbonate saturation state, two processes known as ocean acidification (OA) (Doney et al. 2009; Gattuso et al. 2015; IPPC 2014). Future projections suggest there will be a pH reduction of 0.3 units by the year 2100, threatening marine organisms that produce calcium carbonate exoskeletons and shells, such as corals, molluscs and echinoderms (Kroeker et al. 2010; Hendricks et al. 2010; Hofmann et al. 2010; Widdicombe and Spicer 2008; Wittmann and Pörtner 2013). Because they do not compensate for acid-base disturbances, molluscs are considered to be among the most vulnerable invertebrates with respect to OA, with a pronounced sensitivity in larval and juvenile stages (Beniash et al. 2010; Gazeau et al. 2013; Melzner et al. 2009; Orr et al. 2005; Przeslawski et al. 2015, Ross et al. 2011). In marine shelled molluscs, OA has been shown to reduce larval survival, lengthen development time, alter morphology and/or impair shell formation and calcification (Byrne et al. 2011; Duquette et al. 2017; Ellis et al. 2009; Fitzer et al. 2014a; Gazeau et al. 2010; Kurihara 2008; Noisette et al. 2014). Since many mollusc species are sources of

commercially important foods, negative impacts of OA may also result in significant economic loss (Ekstrom et al. 2015; Gazeau et al. 2007).

Abalone are ecologically and economically important shelled gastropods, which are grazers in the marine ecosystem and a food delicacy for humans (Cook 2014; Huchette and Clavier 2004). Many abalone species worldwide have experienced severe population decline due to both overfishing and environmental perturbations, such as global warming and disease (Nicolas et al. 2002; Travers et al. 2009). In the context of the growth of worldwide aquaculture (Cook 2014), understanding the effects of stress on abalone physiology would allow the farmers to adapt their practices to minimize stress, prevent mortalities and produce higher quality shellfish (Morash and Alter 2015).

The abalone *Haliotis tubercula* is a commercially important species, for which rearing over the whole life cycle is controlled in aquaculture (Courtois de Viçose et al. 2007). It displays a pelago-benthic life cycle with a larval planktonic stage followed by a critical metamorphosis into the benthic juvenile, making this species highly sensitive to environmental changes (Byrne et al. 2011). Several studies have focused on early life-history stages of abalone, especially on larvae, and have demonstrated adverse effects of elevated CO_2, such as reduced survival, developmental delay, body and shell abnormalities and reduction in mineralization (Byrne et al. 2011; Crim et al. 2011; Guo et al. 2015; Kimura et al. 2011; Onitsuka et al. 2018; Wessel et al. 2018; Zippay and Hofmann 2010). Shell formation has been extensively studied in *H. tuberculata*, revealing that aragonite is the main $CaCO_3$ polymorph (Auzoux-Bordenave et al. 2010, 2015). Since aragonite is a less stable polymorph than calcite and is likely to be more susceptible to dissolution (Morse et al. 2007), the abalone shell is expected to be more sensitive to OA (Gazeau et al. 2013). The juvenile stage is a relevant model to study the effects of OA since (i) it corresponds to the growing stage between larvae and adults and (ii) it is a critical period where abalone are submitted to strong predation (Shepherd 1973). So far, only two studies investigated the responses of juvenile abalone to decreased

seawater pH. In juvenile *Haliotis iris* from New Zealand, significant reduction of shell growth was observed under lower pH (0.3 to 0.5 pH units less than the control), but no effect on respiration rate (Cunningham et al. 2016). More recently, the effects of low pH (- 0.3 to - 0.5 units below control pH) on juvenile *H. discus hannai* resulted in eroded shell surfaces, reduced growth rates and altered biochemical composition and energy metabolism (Li et al. 2018). The impact on shell microstructure or resistance to fracture was not investigated.

The goal of the present study was to investigate the effects of CO_2-induced ocean acidification on survival, growth and shell mineralization and mechanics of juveniles of the European abalone *H. tuberculata*. Six-month-old juvenile abalones were cultured for three months under current and near-future pH conditions (8.1, 7.8, 7.7 and 7.6). Biological responses such as survival rate, growth performance (shell length, weight and shell growth) and shell biomineralization were compared across the different pH treatments. SEM microscopy and fracture force analyses were performed to assess whether reduced pH has an influence on shell microstructure, thickness and resistance.

Materials and methods

Abalone collection and rearing

Farmed, 6-month-old juvenile abalones *H. tuberculata* (n = 540 in total, 6.0 ± 0.5 mm total shell length) were collected from nursery tanks at the France Haliotis abalone farm (48°36'46N, 4°33'30W; Plouguerneau, France) in January 2013 and transported to the laboratory at the marine station, Concarneau (MNHN, France). The abalone were randomly distributed into 12 experimental aquaria (12 L) supplied with filtered 3µm natural seawater renewed at a rate of 6 $L.h^{-1}$ and aerated with ambient air. Temperature was the local value in January, i.e., 9.3°C ± 0.5 °C. Animals were conditioned in the laboratory, at ambient pCO_2, at

a density of 45 abalones per aquarium, for 3 weeks. Juvenile abalone shells usually have a green coloration, resulting from their grazing on *Ulvella sp.* algae at the farm. At the start of the experiment, the abalone diet was changed from green algae *Ulvella* to red *Palmaria palmata* which is a high quality alga giving the best growth performance for *H. tuberculata* (Mercer et al. 1993). This changeover is part of standard procedure in aquaculture when juveniles reach 6–10 mm and results in a change of shell colouration from greenish to red (Marchais et al. 2017). Shell maerking by algal feeding can be used as a proxy to determine growth in long term stock enhancement program (Gallardo et al. 2003). This transition allowed us to mark the start (T0) of the experimental period for the evaluation of shell growth. The abalones were fed once a week *ad libitum* with the red macroalgae *Palmaria palmata*.

Experimental design

Experiments were carried out between March and June 2013 at the Concarneau marine station (France) according to an experimental design adapted from Martin et al. (2011). Juvenile abalones were exposed to four pH levels (Total scale) for 3 months. The treatments consisted of a control at present-day pH, pH_T 8.1 ($pCO_2 \approx 400$ µatm), and three levels of predicted pH_T according to different climate change scenarios, as outlined in Riebesell et al. (2010): 7.8 ($pCO_2 \approx 750$ µatm), 7.7 ($pCO_2 \approx 1000$ µatm) and 7.6 ($pCO_2 \approx 1400$ µatm). Three replicate aquaria were set up per pH treatment.

pH control and carbonate chemistry

Low seawater pH_T levels were obtained by bubbling CO_2 (Air Liquide, France) into three 100 L header tanks supplied with filtered through-flowing seawater, continuously aerated with ambient air. Each header tank supplied three experimental 12 L aquaria at a rate of 6 $L.h^{-1}$. pCO_2 in each tank was regulated through electro-valves controlled by a pH-stat system (IKS Aquastar, Germany). pH values of the IKS system were adjusted from daily measurements of the electromotive force (emf) in each aquarium using a pH meter (Metrohm 826 pH mobile, Metrohm, Switzerland) with a glass electrode (Metrohm electrode plus), converted to total scale pH units (pH_T) using Tris/HCl and 2-aminopyridine/HCl buffers (Dickson 2010). At the start of the experiment, pH was gradually decreased over 10 days by 0.05 pH $unit.day^{-1}$ until the different target pH levels were reached.

Seawater parameters were monitored throughout the 3-month experiment. Temperature and pH_T were recorded almost daily in each of the 12 experimental aquaria using a pH meter as described above. Salinity was measured twice a week using a conductivity meter (3110, WTW, Germany). Total seawater alkalinity (A_T) was measured every two weeks on 100 mL samples taken from each experimental aquarium. Seawater samples were filtered through 0.7 µm Whatman GF/F membranes, immediately poisoned with mercury chloride and stored in a cool dark place pending analyses. A_T was determined potentiometrically using an automatic titrator (TitroLine alpha, Schott SI Analytics, Germany), calibrated with the National Bureau of Standards scale. A_T was calculated using a Gran function applied to pH values ranging from 3.5 to 3.0, as described by Dickson et al. (2007), and corrected by comparison with standard reference material provided by Andrew G. Dickson (CRM Batch 111). Seawater carbonate chemistry, i.e., dissolved inorganic carbon (DIC), pCO_2 and aragonite saturation state ($\Omega_{aragonite}$) were calculated from pH_T, A_T, temperature and salinity with the CO_2SYS

program (Pierrot et al. 2006) using constants from Mehrbach et al. (1973) refitted by Dickson and Millero (1987).

Juvenile survival and sampling

Survival of the juvenile abalones was assessed almost daily during the 3-month experiment. Any dead individuals were removed from the tanks immediately. Mortality was calculated as the proportion of the number of dead abalones vs the total number of abalones per tank and then averaged over the three replicates to calculate the mean survival for each pH treatment. Juvenile individuals were sampled at the start of the experiment (T0) and after 3 months of exposure (T3m). Soft tissues were dissected while shells were rinsed with distilled water, dried and stored at room temperature until analysis.

Biometric measurements

Shell length was measured with a Vernier calliper to the nearest 0.05 mm on 12 abalones from each replicate (n = 36 per pH treatment). Shell dry weight was measured on an analytical laboratory balance (Ohaus, Switzerland) to the nearest 0.001 mg (n = 21 per pH treatment, except for pH 7.6, n = 13). For shell weight, the lower number of individuals in pH_T 7.6 is due to the high percentage of broken shells in this condition; indeed, only the whole shells were used for shell weight determination and further SEM analysis on cross sections. The remaining shell samples were used for shell strength measurements. Shell index was calculated as the ratio total shell weight/(shell length)^3 (n = 21 per pH treatment , except for pH 7.6, n = 13).

For the estimation of relative shell growth, the external mark on the shell induced by the change in algal diet (Fig. 1) was used as a proxy to estimate the shell area newly formed during the 3-month experiment. Shell surfaces were examined under a binocular microscope (Leica, Germany) and imaged with NIS elements software (Nikon, Japan). For the determination of relative shell growth, the newly formed area (red coloured) was measured by tracing its outline using Image J software. The ratio of red shell area/total shell area was calculated for each abalone shell and used as a proxy to determine relative shell growth (n = 36 per pH treatment). All measurements were made by a single researcher, with the origin of each shell anonymised to eliminate subjective bias.

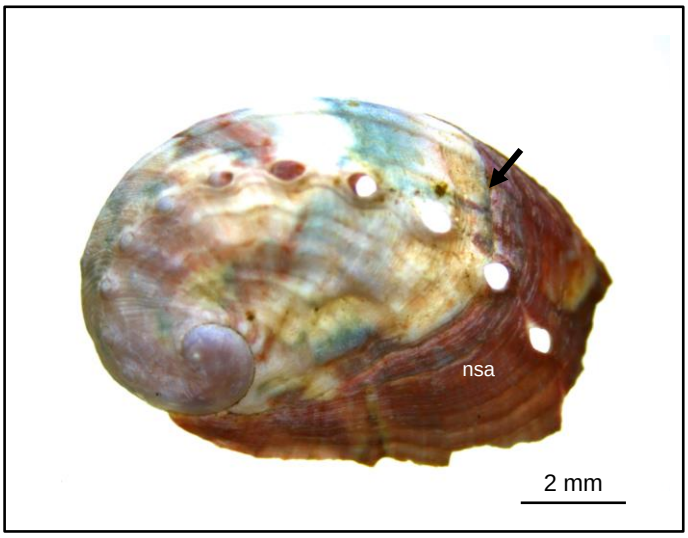

Fig. 1 Shell of a 9-month-old abalone showing the transition from greenish to red colouration induced by the change of algal diet (black arrow); the transition mark was used as a proxy to estimate the shell area newly (nsa) formed during the 3-month experiment.

Scanning electron microscopy (SEM)

Randomly chosen abalone shells from control pH and pH 7.6 (n = 5 per pH treatment) were analysed by SEM. Outer and inner shell surfaces were investigated on whole, gold-coated

(JEOL JFC 1200 fine coater) samples. Shell thickness and microstructure were examined on shell cross-sections cut using a razor blade along the longitudinal growth axis of the shell. Samples were gold-coated (JEOL JFC 1200 fine coater) and observed at 5–15 kV with either a JEOL JSM-840A or a Sigma 300 FE-SEM scanning electron microscope (SEM, Plateau Technique de Microscopie Electronique, MNHN, Paris and Concarneau, France). Shell thickness (total, outer spherulitic and nacre layer thickness) measurements were made on SEM images of the cross sections using Image J software from 6 to 9 transects per shell section (Fig. S1, electronic supplementary material).

Biomechanical tests

Shell strength (resistance) of abalone shells was measured individually (n = 10 shells/pH treatment) using a simple compression method. The shells were placed on a metal block with the opening downwards (i.e., in what would be their natural position on a rocky substrate) and the mechanical test was carried out using a second metal block fixed on the load frame of the force stand (Instron 5543), which was then lowered onto the shell at a speed of 0.3 $mm.min^{-1}$ (simple compression test) until fracture. Displacement and force were recorded continuously at a frequency of 10 Hz using a 100N force cell (Instron 2530-100N). The failure force was recorded for each specimen. A representative curve of compressive force vs displacement is presented in supplementary Fig. S2. A stress-strain relationship was not established because of the absence of symmetry in the abalone shell and the difficulty to define the surface on which the force is applied.

Statistical analysis

All statistical analyses were performed with Rstudio software (R Core Team, 2015). Differences in juvenile survival, shell length and weight, relative growth and shell index across pH treatments were assessed using generalized linear model (GLM) ANOVAs after testing the normality of data, normality of residuals and homogeneity of variances (pH: fixed factor, tank: random factor nested into pH). In the few cases where data distribution deviated from normality and/or variances were not homogeneous, data were Log-transformed to ensure compliance with ANOVA assumptions. If the homogeneity of variance was not verified, a Welch test was performed, as recommended by Day and Quinn (1989). Post-hoc HSD Tukey tests, using the appropriate mean square error, were used to test the differences between the group means. To detect any significant differences in shell thickness, unpaired Student's t-tests were performed. To assess the effect of decreased pH on shell strength, regression analyses were performed to look at the relationships between fracture force and shell weight. ANCOVA model was used to compare linear regression models and evaluate the effect of pH, using weight as a covariate. All data are presented as means ± SD, except where otherwise stated. Differences were considered significant at $P < 0.05$.

Results

Seawater parameters

Mean values of seawater carbonate chemistry parameters for the four pH treatments are given in Table 1. Seawater temperature followed the natural variations found in the bay of Concarneau, ranging from 9.3 ± 0.5°C at the start of experiment (early March) to 16.1 ±

0.5°C at the end (mid-June), with the mean ranging from 12.1 ± 1.8°C to 12.4 ± 1.8°C according to treatment. The pH_T of the experimental aquaria was maintained close to the nominal values throughout the experiment, at pH_T = 8.10 (pCO_2 = 347 ± 5 µatm), pH_T = 7.81 (pCO_2 = 746 ± 10 µatm), pH_T = 7.73 (pCO_2 = 934 ± 13µatm) and pH_T = 7.65 (pCO_2 = 1157 ± 35 µatm). Mean total alkalinity (A_T) measured in the experimental aquaria ranged from 2305 ± 28 $\mu Eq.kg^{-1}$ to 2312 ± 30 $\mu Eq.kg^{-1}$ (n= 8 per pH treatment) over the course of the experiment and presented only slight differences between treatments. Salinity was 35.2 ± 1.7 in all experimental aquaria. $\Omega_{calcite}$ was always greater than 1 in all four pH treatments, while $\Omega_{aragonite}$ only reached values below 1 in the lowest pH_T treatment (7.6).

Survival

The mortality of juvenile abalones was very low, with a survival percentage ranging between 90.9 ± 10.3% and 96 ± 3.3% at the end of the experiment. There were no significant differences in survival among the four pH treatments (ANOVA, $F(3,8) = 0.367$, $P = 0.78$).

Shell growth

Abalones grew in all treatments, from 6.0 ± 0.5 mm at the start of the experiment to 8.3 ± 1.0 mm (pH_T 8.1), 8.7 ± 1.0 mm (pH_T 7.8), 8.1 ± 1.0 mm (pH_T 7.7) and 7.8 ± 1.1 mm (pH_T 7.6) after 3 months. Total shell length after 3 months differed significantly according to pH treatment (ANOVA, $F(3,8) = 4.78$, $P = 0.034$, Fig. 2): juveniles exposed to pH_T 7.6 were significantly smaller than those exposed to pH_T 7.8 (Post-hoc Tukey, $t8 = -3.656$, $P = 0.027$, Table 2). No significant differences were observed between juveniles exposed to pH_T 7.7, 7.8 and the control pH_T (8.1).

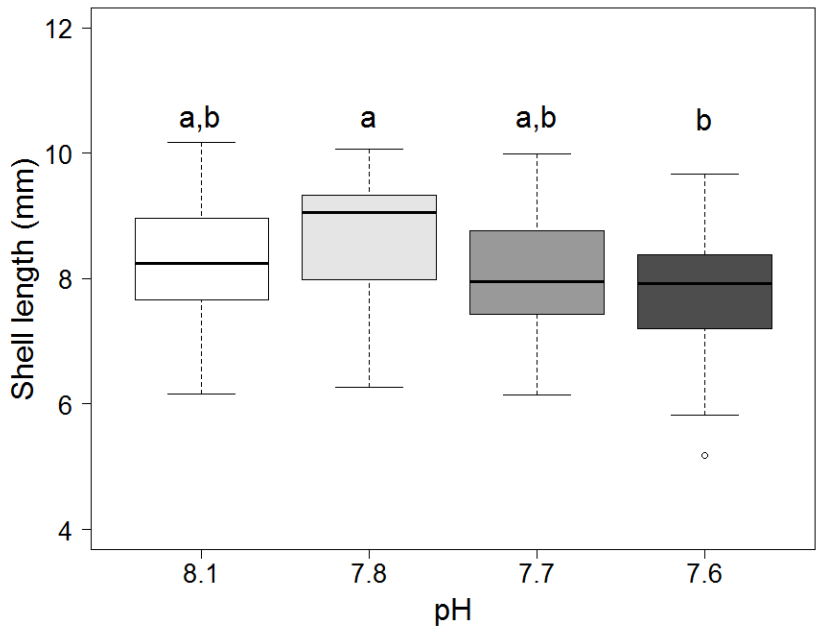

Fig. 2 Shell length of juvenile abalones *H. tuberculata* exposed to decreased pH_T values. Centre lines of box plots show the medians; box limits indicate the first and third quartiles, respectively, with whiskers encompassing data within 1.5 times the spread from the median (n = 36 per pH treatment). Different letters indicate significant differences between pH treatments ($P < 0.05$).

Shell weight was significantly affected by pH (ANOVA, $F(3,8) = 24.43$, $P < 0.001$, Fig. 3), being lower for juveniles exposed to pH_T 7.6 compared with those grown in other pH treatments (Post-hoc Tukey, $P < 0.005$, Table 2). Relative shell growth, determined as the ratio of red shell area/total shell area, did not differ significantly between pH treatments (ANOVA, $F(3,8) = 0.626$, $P = 0.618$, Table 2).

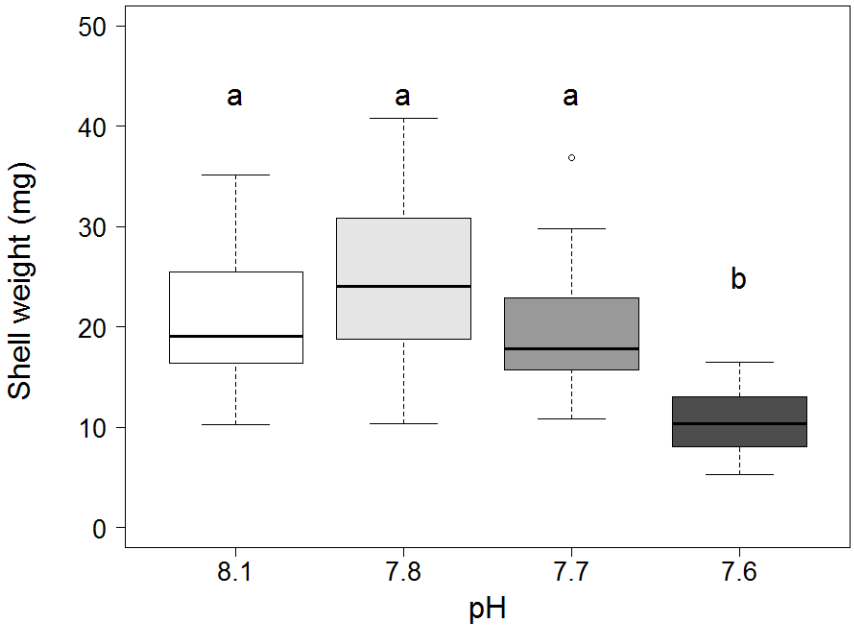

Fig. 3 Shell weight of juvenile abalones *H. tuberculata* exposed to decreased pH_T values. Centre lines of box plots show the medians; box limits indicate the first and third quartiles respectively, with whiskers encompassing data within 1.5 times the spread from the median (n = 22 per pH treatment, except for pH 7.6 n = 13). Different letters indicate significant differences between pH treatments ($P < 0.05$).

Shell calcification

Shell index was significantly affected by pH (Welch's F-test, $F(3, 3.982) = 14.48$, $P = 0.013$; Fig. 4). Abalones in the pH_T 7.6 treatment had a reduced shell index compared to those grown in the other pH treatments ($P < 0.005$, Table 2).

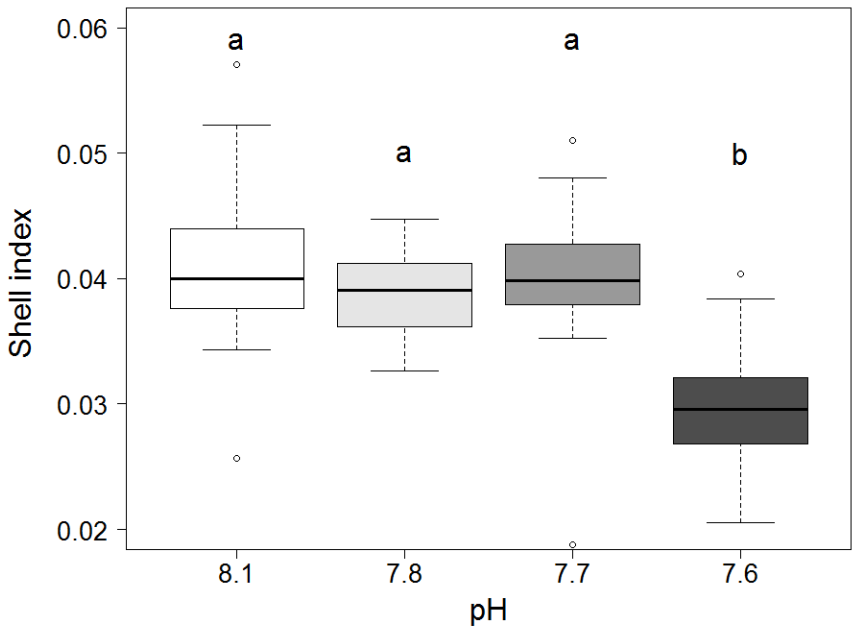

Fig. 4 Shell index (determined as the ratio shell weight/shell length^3) of juvenile abalones under different pH_T conditions. Centre lines of box plots show the medians; box limits indicate the first and third quartiles, respectively, with whiskers encompassing data within 1.5 times the spread from the median (n = 22 per pH treatment, except for pH_T 7.6 n = 13). Different letters indicate significant differences between pH treatments ($P < 0.05$).

SEM examination of abalone shells grown at pH_T 8.1 and 7.6 revealed differences in the texture and porosity of both outer and inner surface layers. Under control conditions, almost intact periostracum were observed with typical ornamentations (ridge and groove pattern)and regular organic sheets (Fig. 5a, c). At lower pH, the periostracum revealed bleached areas and a corroded surface with numerous small holes (Fig. 5b, d). In some individuals, large holes were observed between the apertures as the result of shell corrosion (Fig. 5b). The delamination of surface organic sheets revealed biominerals of the underlying spherulitic layer (Fig. 5d). In control shells, the inner nacreous layer had a homogeneous surface, with a gradual maturation of aragonite platelets (Fig. 6a, c, e). By contrast, juvenile shells from the low pH treatment (pH 7.6) were characterized by a partial degradation of the inner nacreous

355 layer, resulting in decreased size of aragonite platelets and irregularities of their edges (Fig.
356 6b, d, f).
357

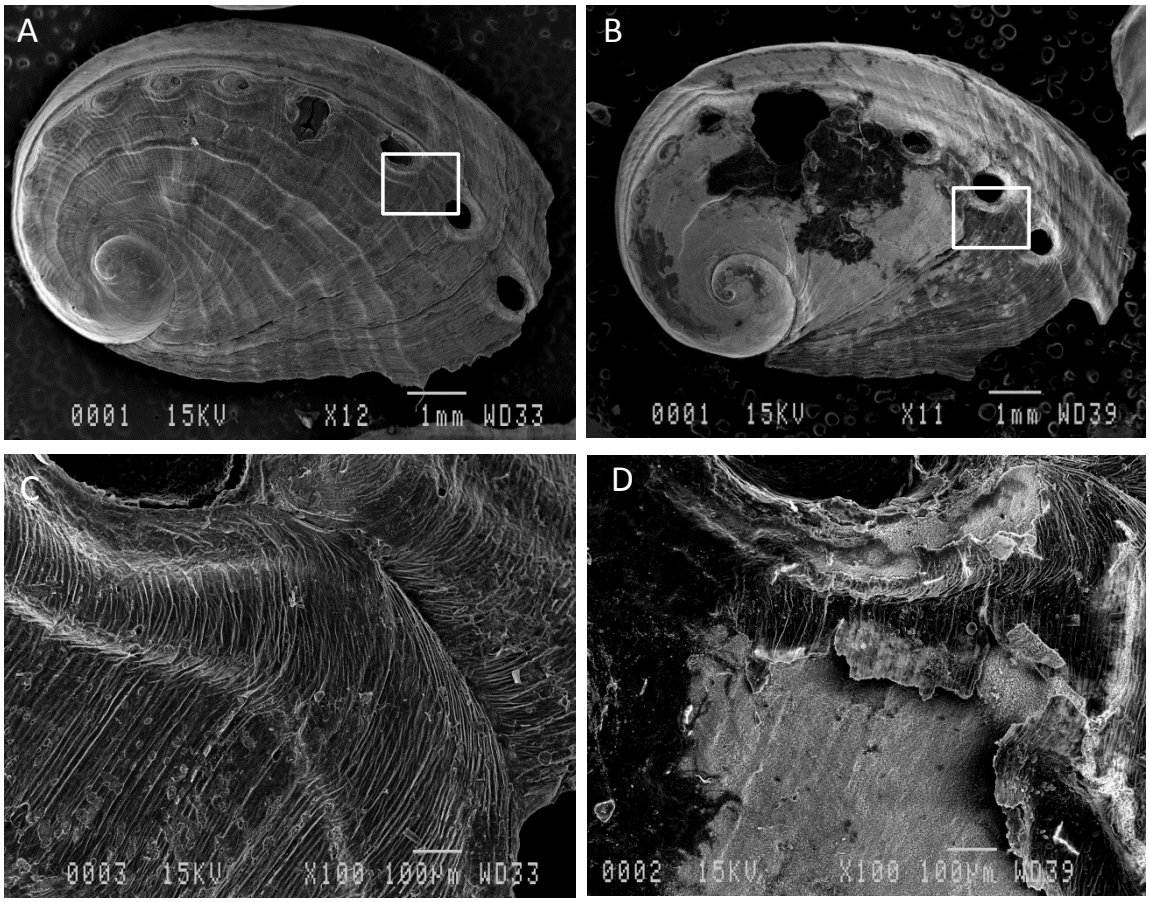

358

359 **Fig. 5** SEM images of abalone outer shell surface in control conditions (pH_T 8.1: A, C) and
360 under lower pH (pH_T 7.6: B, D). **A**. Periostracum in the control, showing a homogenous
361 surface with the typical ridge and groove patterns; **B**. Periostracum in the pH_T 7.6 treatment,
362 showing bleached areas and corroded surface; **C.** Detail of the shell area boxed in A, showing
363 regular organic sheets; **D.** Detail of the shell area boxed in B, showing the delamination of
364 organic sheets and revealing biominerals of the underlying spherulitic layer.

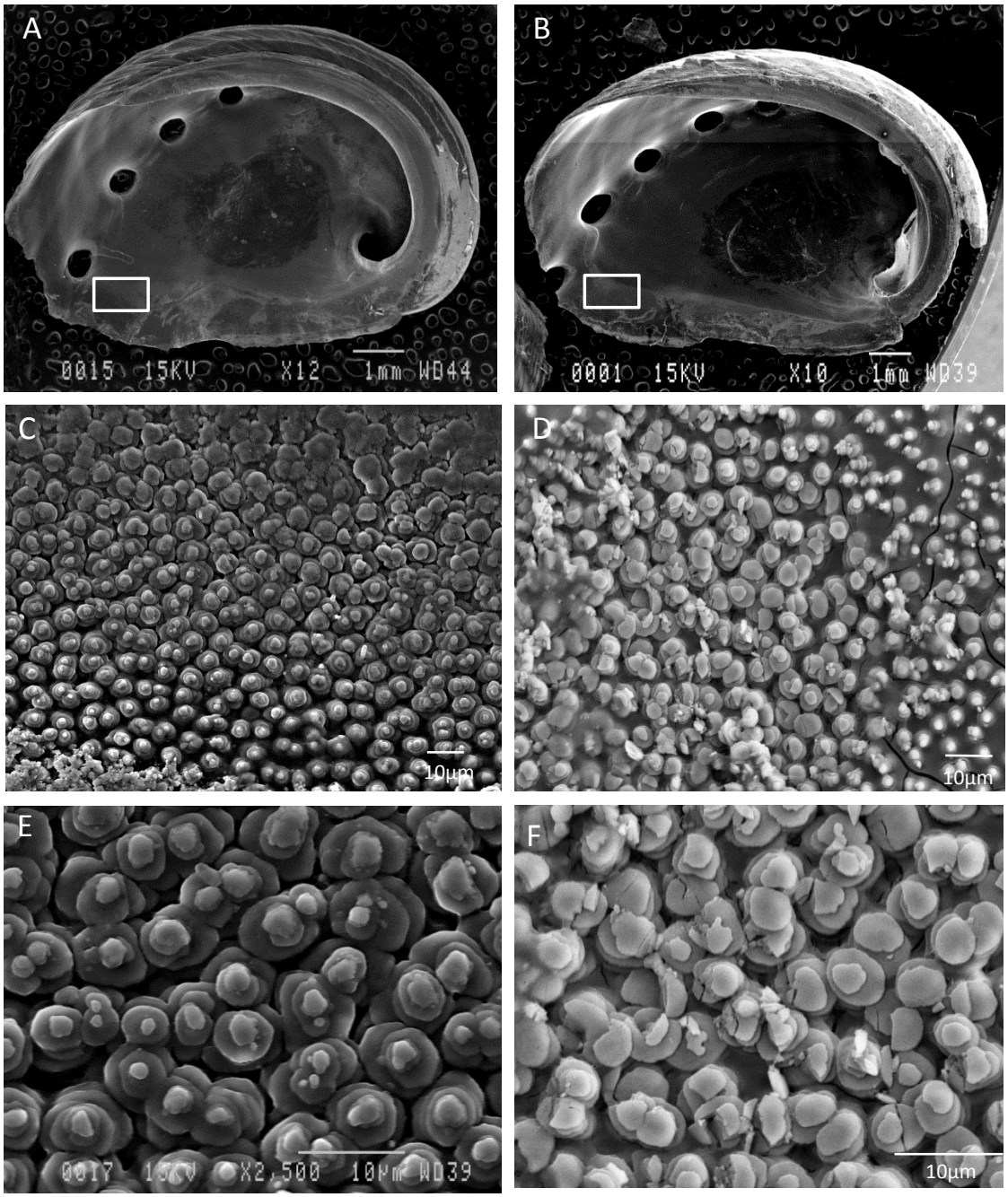

365

366 **Fig. 6** SEM images of abalone inner nacreous surface in control conditions (pH_T 8.1: A, C, E)
367 and under low pH_T 7.6 (B, D, F). **A.** Inner nacreous layer of control shell; **B.** Inner nacreous
368 layer of shell exposed to pH_T 7.6; **C.** Detail of the nacre growth region boxed in A showing
369 gradual maturation of aragonite platelets; **D.** Detail of the nacre surface boxed in B showing
370 disruption of the aragonite platelets; **E.** Magnification of the nacre surface showing
371 confluence of regular aragonite platelets; **F.** Magnification of the nacre platelets showing
372 breaks within the platelets and irregularities of their edges.

Measurements along the shell section showed a progressive decrease of total shell thickness from older to newly formed shell regions (results not shown), which is in accordance with the shell growth process. Total shell thickness tended to be smaller in juveniles exposed to pH 7.6 compared with those reared under control pH_T (unpaired t test, $t8 = -2.1644$, $P = 0.062$, Fig. 7a). However, a significant reduction of the spherulitic layer thickness was observed at pH_T 7.6 compared with the control group (unpaired t test, $t8 = -2.8522$, $P = 0.021$, Fig. 7b). There was no significant differences in nacre shell thickness between abalones grown in these two pH treatments (unpaired t test, $t8 = -0.4381$, $P = 0.67$).

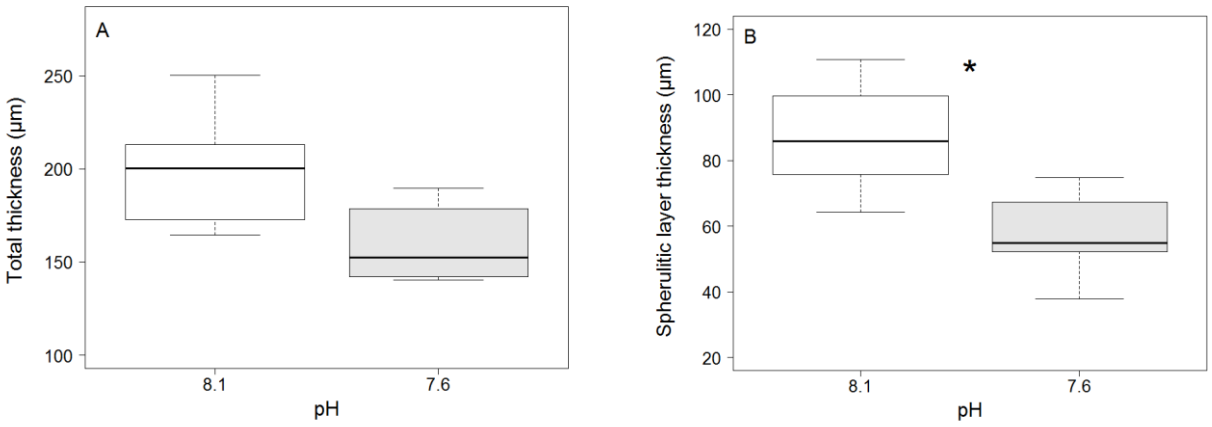

Fig. 7 Total thickness (A) and spherulitic layer thickness (B) of juvenile abalone shells grown under control pH_T (8.1) and low pH_T (7.6) treatment. Centre lines of box plots show the medians; box limits indicate the first and third quartiles, respectively, with whiskers encompassing data within 1.5 times the spread from the median (n = 5 per pH condition). Asterisk indicates a significant difference between pH treatments (unpaired Student's t-test, $P < 0.05$).

The shell fracture force was significantly lowered at pH_T 7.6 compared with shells that had grown in the three other pH treatments (ANOVA, $F(3,7) = 11.15$, $P = 0.0047$, Fig. 8, Table 3). However, because shell weight (and thickness) was reduced at low pH, the fracture force was analysed according to weight. The regression of shell fracture force on abalone shell

weight showed a linear relationship (Linear regression, $r^2 = 0.63$, $F(1,41) = 68.42$, $P = 0.031$, Fig. 9). A test of homogeneity of slopes of the regression lines of shell fracture force vs weight showed that these were not significantly different between pH treatments (interaction pH * weight, $F(3,34) = 0.486$, $P = 0.69$, Table 4). Testing on the intercept with shell weight as a co-variable, showed that the effect of pH on shell fracture force was not significant (ANCOVA, $F(3,7) = 1.021$, $P = 0.44$). This indicates that the decreased fracture force at pH_T 7.6 could be explained by the reduced amount of shell material only.

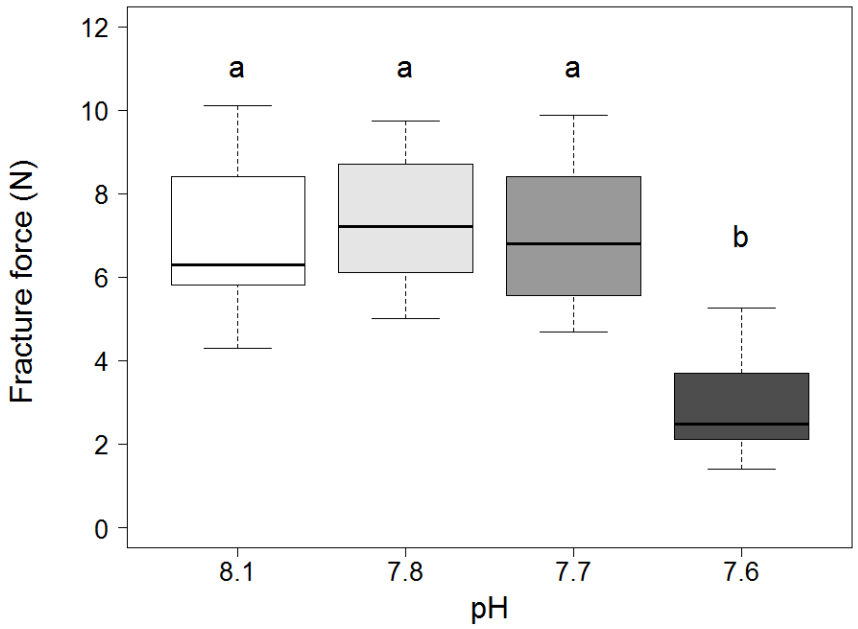

Fig. 8 Fracture force of the shells of abalones reared under different pH conditions. Centre lines of box plots show the medians; box limits indicate the first and third quartiles, respectively, with whiskers encompassing data within 1.5 times the spread from the median (n = 12 for pH_T 8.1 and 7.8; n = 11 for pH_T 7.7; n = 7 for pH_T 7.6). Different letters indicate significant differences between pH treatments ($P < 0.05$).

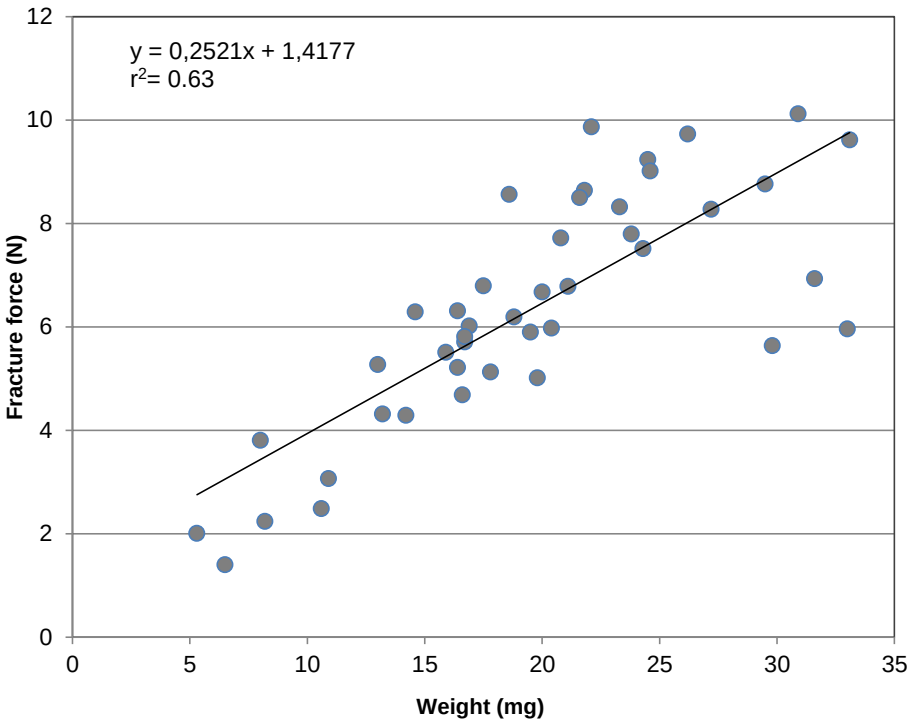

Fig. 9 Linear regression of shell fracture force against abalone shell weight (n = 43) (r^2 = 0.63, $F(1,41)$ = 68.42, P = 0.031).

Discussion

The present study demonstrated that decreased pH negatively impacts the growth and shell mineralization of juvenile European abalone *Haliotis tuberculata.* Almost all the tested variables were significantly reduced at pH_T 7.6 (0.5 units below control pH) while pH_T 7.7 and 7.8 did not affect juvenile growth. These results are rather similar to those obtained in two other species of farmed abalone. In juvenile *H. iris*, Cunningham et al. (2016) reported significant effects on shell length and wet weight at pH_{NBS} 7.6 in winter (corresponding to pH_T 7.5) and at pH_{NBS} 7.8 (pH_T 7.7; 0.3 units below control pH) and 7.6 (pH_T 7.5; 0.5 units below control pH) in summer. Similarly, shell growth and shell weight were significantly lower in juvenile *H. discus hannai* after 3 months of exposure to pH_{NBS} 7.7 and 7.9 (corresponding respectively to pH_T 7.8 and 7.6, Li et al. 2018). These results are also in

443 accordance with previous studies on other marine shelled mollusc taxa, showing significant
444 reductions in shell growth following medium to long term exposure to near-future pH
445 (reviewed in Gazeau et al. 2013). In a two-month experiment, Thomsen and Melzner (2010)
446 observed significant decreases in both shell mass and shell length in blue mussels exposed to
447 lowered pH (- 0.3 to - 0.9 units). Similarly, the mussel *Mytilus galloprovincialis* exhibited a
448 slow-down of shell growth when pH was reduced by 0.75 units, possibly caused by
449 dissolution (Michaelidis et al. 2005). As suggested in previous studies, the effects of OA on
450 shell growth and calcification would result either from a direct effect on $CaCO_3$ dissolution or
451 from indirect metabolic effects, such as physiological and molecular processes regulating
452 shell biomineralization (Beniash et al. 2010; Hüning et al. 2012; Klok et al. 2014). The
453 increasing cost of maintaining acid-base balance combined with an impaired ability to calcify
454 under OA may explain the decrease in the scope for growth among early life stages of
455 molluscs experiencing acidified conditions (Gazeau et al. 2013; Parker et al. 2013; Thomsen
456 et al. 2015). However, Cunningham et al. (2016) found no changes in respiration rate of *H.*
457 *iris* juveniles subjected to reduced pH (- 0.3 to - 0.5 units), indicating that abalone do not up-
458 regulate their metabolism. Nothing is known on the acid-base balance regulation abilities of
459 abalones but molluscs (apart from cephalopods) are usually considered to have a poor ability
460 to compensate for decreasing haemolymph pH in situations of seawater acidification (Melzner
461 et al. 2009). According to Cyronak et al. (2016), elevated H^+ concentration and subsequent
462 problems of homeostasis rather than carbonate ions concentration, would be more likely
463 responsible for the reduction of calcification in marine organisms facing OA.

464 Our results revealed significant changes in shell microstructure of juvenile abalones grown
465 at pH_T 7.6, including corrosion of the outer periostracum and degradation of the inner
466 nacreous aragonite layer. In juvenile *H. discus hannai*, corroded periostracum was found in
467 individuals grown at pH_{NBS} 7.7 (Li et al. 2018), but the effect of decreased pH on shell
468 microstructure was not investigated. Shell surface corrosion and changes in biomineral

microstructure under low pH have been previously reported in juvenile bivalves and related to a direct effect on shell dissolution (Fitzer et al. 2014b; Hiebenthal et al. 2013; McClintock et al. 2009; Melzner et al. 2011; Waldbusser et al. 2011). It is noteworthy that we only recorded significant effects at pH_T 7.6, the only treatment at which $\Omega_{aragonite}$ was lower than one. The corrosion of the periostracum and degradation of the nacreous layer were observed both in the old part and in the newly formed shell under the low pH, indicating that direct dissolution is involved rather than indirect metabolic process affecting the synthesis of the new shell. However, the energetic cost for proton elimination during $CaCO_3$ precipitation is increased under elevated pCO_2, suggesting a metabolic effect.

This finding also supports the hypothesis that the effects on shell length and weight may be mainly due to the shell dissolution. Indeed, the juvenile and adult shells of *H. tuberculata* consist of two biomineralized layers, the outer spherulitic and the inner nacreous layers, both composed of the aragonite $CaCO_3$ polymorph (Auzoux-Bordenave et al. 2010, 2015; Jardillier et al. 2008). The predominance of aragonite in the *H. tuberculata* shell makes the species more susceptible to dissolution than other mollusc species with calcitic shells or a calcite/aragonite mixture (Gazeau et al. 2013; Parker et al. 2013). In the course of a trans-generational experiment on juvenile *M. edulis* exposed to elevated pCO_2, Fitzer et al. (2014a) revealed that mussels at high pCO_2 (1000µatm) did not produce aragonite, which is more vulnerable to carbonate under-saturation than calcite. Under lower pCO_2 (550, 750 µatm), the nacreous tablets formed the usual 'brick wall' structure, although the nacre crystals appeared corroded and were not so closely stacked together as under normal conditions (Fitzer et al. 2014a). This could indicate reduced biological control over biomineralization of aragonite by the organism and potentially raises questions about the integrity of mollusc shells composed only of aragonite under OA.

In addition to changes in shell microstructure, we found a significant reduction in the spherulitic shell thickness and, to a lesser extent, in the total thickness of abalone shells grown

495 at pH_T 7.6. The reduction of shell thickness is likely due to $CaCO_3$ dissolution of the outer
496 aragonite layer, which would be more sensitive to OA after periostracum corrosion. In
497 juvenile shells of *M. edulis*, a reduction in shell thickness was reported in the aragonite layer,
498 but not in the calcite layer, after 6 months of exposure to elevated pCO_2 (Fitzer et al. 2014b).
499 Other juvenile bivalves (*Argopecten irradians* and *Mercenaria mercenaria*) grown under
500 increased CO_2 concentration (corresponding to a reduction of 0.4 to 0.6 pH units), also
501 exhibited malformed and corroded shells with reduced thickness (Talmage and Gobler 2010).
502 Welladsen et al. (2010) also reported a significant decrease in shell strength and nacre
503 malformation in the adult pearl oyster *Pinctada fucata* exposed to acidified seawater (pH_{NBS}
504 7.6), suggesting shell dissolution.

505 The integrity of the periostracum (the organic coating of the mollusc shell) is very
506 important for protecting the shell from corrosion induced by low pH (Thomsen et al. 2010). In
507 juvenile abalone, we found that the periostracum was damaged under low pH, resulting in a
508 higher vulnerability of the underlying mineralized layers. Indeed, a subsequent reduction in
509 thickness of the spherulitic layer as well as changes in the nacreous layer microstructure were
510 observed. These observations are consistent with those reported for other shellfish reared
511 under lowered pH (Talmage and Gobler 2010). All of this suggests that processes leading to
512 the synthesis of the periostracum are affected by low pH, implying that the kinetics of
513 aragonite precipitation (evidenced by the reduced growth rate) and the thermodynamics of its
514 dissolution (due to under saturated sea water in the pH_T 7.6 treatment) are not the only aspects
515 of the shell being affected. Potential effects of decreased pH on shell organic components
516 (chitin and matrix proteins) may explain the corrosion of the periostracum and some of the
517 changes observed in the nacre microstructure, but the underlying mechanisms are far from
518 being understood (Fitzer et al. 2014b; Hüning et al. 2012). A number of indirect biological
519 processes involved in shell calcification, such as matrix protein production, chitin synthesis
520 and enzymatic control are influenced by changes in seawater pCO_2 (Weiss et al. 2013). In the

mussel *M. edulis*, six months of incubation at 750 µatm pCO_2 (pH_T 7.5) significantly reduced carbonic anhydrase activity within the mantle tissue, explaining shell growth reduction (Fitzer et al. 2014b). In another study of *M. edulis*, a strong depression in the expression of mRNA for a chitinase, an enzyme involved in the calcification process, was correlated with a linear decrease in shell growth (Hüning et al. 2012). Interestingly, this study also found that expression of several genes, including some genes involved in shell protection and/or periostracum formation (tyrosinase) increased in response to elevated pCO_2 (Hüning et al. 2012). By contrast, despite evidence of shell dissolution, no difference was found in the organic content or periostracum integrity of adult *P. fucata* shells exposed to pH_{NBS} 7.6 (Welladsen et al. 2010). However, the authors noted that because the study was conducted over only a 28-day period, it did not allow acclimation of the oysters to the acidified conditions.

In juvenile *H. tuberculata*, the significant reduction in shell fracture force at pH_T 7.6 can be explained by the reduced shell weight. This probably results from both reduced growth and shell dissolution. A smaller (isometric) dome is submitted to a higher meridional compressive stress for the same external force applied and will therefore rupture at a lower applied force (Vogel 2003). Shell dissolution will induce an easier induction of cracks and cleavage, probably initiated by dissolution pits inducing stress concentration at their level (Mc Neill 1968). Both effects would increase the period during which abalone are exposed to strong predation pressure before they reach a refuge in size and shell strength. This would have an economic impact on abalone aquaculture as it would increase the time required to reach a marketable size and possibly enhance productivity losses through shell breakage during handling.

Marine molluscs exert a strong control on the calcification process, but their capacities to maintain optimal conditions at the site of calcification when facing OA stress remain largely unknown (Gazeau et al. 2013; Parker et al. 2013). Because shell calcification has a high energetic cost and is very sensitive to OA (especially in early stages), energy usually allocated

547 to growth and reproduction might be partially reallocated to calcification (Thomsen and
548 Melzner 2010). The capacity of abalone to grow in the near future will depend on their
549 potential to maintain their vital functions (reproduction, growth and biomineralization) under
550 modified environmental conditions. Since responses to OA may also differ according to
551 differences in physiology, habitat and behaviour of the species (Gazeau et al. 2013), the local
552 seasonal variations in physico-chemical conditions should be considered in further studies on
553 adaptive responses. The seawater pH_T along the Brittany coast in France naturally varies from
554 7.9 to 8.2 (Qui-Minet et al. 2018), so that a future scenario testing a decrease of - 0.3 units
555 from ambient pH_T is consistent with seasonal or diurnal variations presently experienced by
556 abalone in the tidal zone. Indeed, seasonal variations in pH are close to 0.3 units in shallow
557 subtidal environments (Qui-Minet et al. 2018), while diurnal variations of pH_T in the intertidal
558 zone can be higher. For instance, pH can fall down to pH_T 7.5 in rock pools along the Brittany
559 coast during night-time emersion at low tide (Legrand et al. 2018). Thus, abalone from
560 Brittany shoreline environments might already experience chronically pH similar to global
561 average pH levels predicted for open ocean by 2100 (ie. pH_T 7.7). Such fluctuations of pH in
562 their coastal habitats might explain the potential resistance of abalone to $pH_T > 7.6$.

563 The results of our study indicate that a decrease of 0.5 pH units significantly reduces
564 growth, shell calcification and shell strength of juvenile abalone *H. tuberculata*. In the natural
565 environment, where juvenile stages are exposed to a strong predation pressure, abalone may
566 be at greater risk under future pH conditions as their shells may not offer sufficient protection
567 from predators and other external stressors. Understanding how different abalone life stages
568 respond to OA will make it possible to identify bottlenecks for population persistence under
569 near-future pH conditions. These findings also highlight the importance of monitoring
570 seawater parameters in aquaculture systems, where effort can be directed to maintaining
571 seawater pH at key periods of abalone culture to minimize stress and prevent production
572 losses.

Acknowledgements

N. Wessel was supported by a postdoctoral fellowship from the MNHN (*Ministère de l'Enseignement Supérieur et de la Recherche*, Paris, France). This work was supported in part by the ATM program "Biomineralization" of the MNHN funded by the *Ministère délégué à l'Enseignement Supérieur et à la Recherche* (Paris, France) and by the ICOBio project under the program "*Acidification des Océans*" funded by the Fondation pour la Recherche sur la Biodiversité (FRB) and the *Ministère de la Transition Ecologique et Solidaire* (MTES). We thank Dr. Chakib Djejat and Stéphane Formosa for their assistance in scanning electron microscopy (SEM, *Plateau technique de Microscopie Electronique*, MNHN, Paris and Concarneau, France). The Regional Council of Brittany, the General Council of Finistère, the urban community of *Concarneau Cornouaille Agglomération* and the European Regional Development Fund (ERDF) are acknowledged for the funding of the Sigma 300 FE-SEM of the Concarneau Marine Station. We thank Dr. Cedric Hubas for his valuable support for the statistical analyses and the Translation Bureau of the University of Western Brittany for improving the English of this manuscript. We also thank the 3 anonymous reviewers for their comments which have helped to improve this manuscript. Ph. Dubois is a Research Director of the National Fund for Scientific Research (Belgium).

Compliance with ethical standards

The authors declare that they have no conflicts of interest or competing financial interests.

The experiments complied with the current French laws. All applicable international, national, and institutional guidelines for the care and use of animals were followed.

References

Auzoux-Bordenave S, Badou A, Gaume B, Berland S, Helléouet M-N, Milet C, Huchette S (2010) Ultrastructure, chemistry and mineralogy of the growing shell of the European abalone *Haliotis tuberculata*. J Struct Biol 171:277–290. doi: 10.1016/j.jsb.2010.05.012

Auzoux-Bordenave S, Brahmi C, Badou A, De Rafélis M, Huchette S (2015) Shell growth, microstructure and composition over the development cycle of the European abalone *Haliotis tuberculata*. Mar Biol 162:687–697. doi: 10.1007/s00227-015-2615-y

Beniash E, Ivanina A, Lieb NS, Kurochkin I, Sokolova IM (2010) Elevated level of carbon dioxide affects metabolism and shell formation in oysters *Crassostrea virginica*. Mar Ecol Prog Ser 419:95–108. doi: 10.3354/meps08841

Byrne M, Ho M, Wong E, Soars NA, Selvakumaraswamy P, Shepard-Brennand H, Dworjanyn SA, Davis AR (2011) Unshelled abalone and corrupted urchins: development of marine calcifiers in a changing ocean. Proc R Soc B Biol Sci 278:2376–2383. doi: 10.1098/rspb.2010.2404

Cook PA (2014) The worldwide abalone industry. Mod Econ 05:1181–1186. doi: 10.4236/me.2014.513110

Courtois de Viçose G, Viera MP, Bilbao A, Izquierdo MS (2007) Embryonic and larval development of *Haliotis tuberculata coccinea* Reeve: an indexed micro-photographic sequence. J Shellfish Res 26:847–854. doi: 10.2983/0730-8000(2007)26[847:EALDOH]2.0.CO;2

Crim RN, Sunday JM, Harley CDG (2011) Elevated seawater CO_2 concentrations impair larval development and reduce larval survival in endangered northern abalone (*Haliotis kamtschatkana*). J Exp Mar Biol Ecol 400:272–277. doi: 10.1016/j.jembe.2011.02.002

621 Cunningham SC, Smith AM, Lamare MD (2016) The effects of elevated pCO_2 on growth,
622 shell production and metabolism of cultured juvenile abalone, *Haliotis iris*. Aquac Res
623 47:2375–2392. doi: 10.1111/are.12684

624 Cyronak T, Schulz KG, Jokiel PL (2016) The Omega myth: what really drives lower
625 calcification rates in an acidifying ocean. ICES J Mar Sci 73: 558–562
626 doi:10.1093/icesjms/fsv075

627 Day RW, Quinn GP (1989) Comparisons of treatments after an analysis of variance in
628 ecology. Ecol Monogr 59:433–463. doi: 10.2307/1943075

629 Dickson AG (2010) Standards for ocean measurements. Oceanography 23:34–47. doi:
630 10.5670/oceanog.2010.22

631 Dickson AG, Millero FJ (1987) A comparison of the equilibrium constants for the
632 dissociation of carbonic acid in seawater media. Deep-Sea Res 34:1733–1743.

633 Dickson AG, Sabine CL, Christian JR (2007) Guide to best practices for ocean CO_2
634 measurements. PICES Spec Publ 3, 191pp.

635 Doney SC, Fabry VJ, Feely RA, Kleypas JA (2009) Ocean acidification: the other CO_2
636 problem. Annu Rev Mar Sci 1:169–192. doi: 10.1146/annurev.marine.010908.163834

637 Duquette A, McClintock JB, Amsler CD, Pérez-Huerta A, Milazzo M, Hall-Spencer JM,
638 (2017) Effects of ocean acidification on the shells of four Mediterranean gastropod
639 species near a CO_2 seep. Mar Pollut Bull 124 : 917-928.
640 https://doi.org/10.1016/j.marpolbul.2017.08.007

641 Ekstrom JA, Suatoni L, Cooley SR, Pendleton LH, Waldbusser GG, Cinner JE, Ritter J,
642 Langdon C, Van Hooidonk R, Gledhill D, Wellman K, Beck MW, Brander LM,
643 Rittschof D, Doherty C, Edwards PET, Portela R (2015) Vulnerability and adaptation of

644 US shellfisheries to ocean acidification. Nat Clim Change 5:207–214. doi:
645 10.1038/nclimate2508

646 Ellis RP, Bersey J, Rundle SD, Hall-Spencer JM, Spicer JI (2009) Subtle but significant
647 effects of CO_2 acidified seawater on embryos of the intertidal snail, *Littorina obtusata*.
648 Aquat Biol 5:41–48. doi: 10.3354/ab00118

649 Fitzer SC, Cusack M, Phoenix VR, Kamenos NA (2014a) Ocean acidification reduces the
650 crystallographic control in juvenile mussel shells. J Struct Biol 188:39–45. doi:
651 10.1016/j.jsb.2014.08.007

652 Fitzer SC, Phoenix VR, Cusack M, Kamenos NA (2014b) Ocean acidification impacts mussel
653 control on biomineralisation. Sci Rep 4:6218. doi: 10.1038/srep06218

654 Gallardo WG, Bautista-Teruel MN, Fermin AC, Marte CL (2003) Shell marking by artificial
655 feeding of the tropical abalone *Haliotis asinina* Linne juveniles for sea ranching and
656 stock enhancement. Aquac. Res. 34, 839-842).

657 Gattuso JP, Magnan A, Bille R, Cheung WWL, Howes EL, Joos F, Allemand D, Bopp L,
658 Cooley SR, Eakin CM, Hoegh-Guldberg O, Kelly RP, Portner HO, Rogers AD, Baxter
659 JM, Laffoley D, Osborn D, Rankovic A, Rochette J, Sumaila UR, Treyer S, Turley C
660 (2015) Contrasting futures for ocean and society from different anthropogenic CO_2
661 emissions scenarios. Science 349:4722–4722. doi: 10.1126/science.aac4722

662 Gazeau F, Quiblier C, Jansen JM, Gattuso J-P, Middelburg JJ, Heip CHR (2007) Impact of
663 elevated CO_2 on shellfish calcification. Geophys Res Lett. doi: 10.1029/2006gl028554

664 Gazeau F, Gattuso JP, Dawber C, Pronker AE, Peene F, Peene J, Heip CHR, Middelburg JJ
665 (2010) Effect of ocean acidification on the early life stages of the blue mussel *Mytilus*
666 *edulis*. Biogeosciences 7:2051–2060. doi: 10.5194/bg-7-2051-2010

667 Gazeau F, Parker LM, Comeau S, Gattuso J-P, O'Connor WA, Martin S, Pörtner H-O, Ross
668 PM (2013) Impacts of ocean acidification on marine shelled molluscs. Mar Biol
669 160:2207–2245. doi: 10.1007/s00227-013-2219-3

670 Guo X, Huang M, Pu F, You W, Ke C (2015) Effects of ocean acidification caused by rising
671 CO_2 on the early development of three mollusks. Aquat Biol 23:147–157. doi:
672 10.3354/ab00615

673 Hendriks IE, Duarte CM, Álvarez M (2010) Vulnerability of marine biodiversity to ocean
674 acidification: A meta-analysis. Estuar Coast Shelf Sci 86:157–164. doi:
675 10.1016/j.ecss.2009.11.022

676 Hiebenthal C, Philipp EER, Eisenhauer A, Wahl M (2013) Effects of seawater pCO_2 and
677 temperature on shell growth, shell stability, condition and cellular stress of Western
678 Baltic Sea *Mytilus edulis* (L.) and *Arctica islandica* (L.). Mar Biol 160: 2073–2087. doi:
679 10.1007/s00227-012-2080-9

680 Hofmann GE, Barry JP, Edmunds PJ, Gates RD, Hutchins DA, Klinger T, Sewell MA (2010)
681 The effect of ocean acidification on calcifying organisms in marine ecosystems: an
682 organism to-ecosystem perspectiv. Annu Rev Ecol Evol Syst 41:127–147. doi:
683 10.1146/annurev.ecolsys.ll0308.120227

684 Huchette S, Clavier J (2004) Status of the ormer (*Haliotis tuberculata* L.) industry in Europe.
685 J Shellfish Res 23 : 951–955.

686 Hüning AK, Melzner F, Thomsen J, Gutowska MA, Krämer L, Frickenhaus S, Rosenstiel P,
687 Pörtner H-O, Philipp EER, Lucassen M (2012) Impacts of seawater acidification on
688 mantle gene expression patterns of the Baltic Sea blue mussel: implications for shell
689 formation and energy metabolism. Mar Biol 160: 1845-1861. doi: 10.1007/s00227-012-
690 1930-9

691 IPCC (2014) Summary for Policymakers. In: Climate Change 2014: Impacts, Adaptation, and
692 Vulnerability. Part A: Global and Sectoral Aspects. Contribution of Working Group II
693 to the Fifth Assessment Report of the Intergovernmental Panel on Climate Change.
694 Cambridge University Press, Cambridge, United Kingdom and New York, NY, USA,
695 pp 1–32

696 Jardillier E, Rousseau M, Gendron-Badou A, Fröhlich F, Smith DC, Martin M, Helléouet M-
697 N, Huchette S, Doumenc D, Auzoux-Bordenave S (2008) A morphological and
698 structural study of the larval shell from the abalone Haliotis tuberculata. Mar Biol, 154
699 (4): 735-744,

700 Kimura RYO, Takami H, Ono T, Onitsuka T, Nojiri Y (2011) Effects of elevated pCO_2 on the
701 early development of the commercially important gastropod, Ezo abalone *Haliotis*
702 *discus hannai*. Fish Oceanogr 20:357–366. doi: 10.1111/j.1365-2419.2011.00589.x

703 Klok C, Wijsman JWM, Kaag K, Foekema E (2014) Effects of CO_2 enrichment on cockle
704 shell growth interpreted with a Dynamic Energy Budget model J Sea Res 94 : 111–116

705 Kroeker KJ, Kordas RL, Crim RN, Singh GG (2010) Meta-analysis reveals negative yet
706 variable effects of ocean acidification on marine organisms. Ecol Lett 13:1419–1434.
707 doi: 10.1111/j.1461-0248.2010.01518.x

708 Kurihara H (2008) Effects of CO_2-driven ocean acidification on the early developmental
709 stages of invertebrates. Mar Ecol Prog Ser 373:275–284. doi: 10.3354/meps07802

710 Legrand E, Riera P, Pouliquen L, Bohner O, Cariou T, Martin S (2018) Ecological
711 characterization of intertidal rockpools: Seasonal and diurnal monitoring of physico-
712 chemical parameters. Reg Stud Mar Sci 17:1–10. doi: 10.1016/j.rsma.2017.11.003

713 Li J, Mao Y, Jiang Z, Zhang J, Fang J, Bian D (2018) The detrimental effects of CO_2-driven
714 chronic acidification on juvenile Pacific abalone (*Haliotis discus hannai*).
715 Hydrobiologia 809, 297-308. https://doi.org/10.1007/s10750-017-3481-z

716 Marchais, V., Jolivet, A., Herve, S., Roussel, S., Schone, B.R., Grall, J., Chauvaud, L.,
717 Clavier, J., 2017. New tool to elucidate the diet of the ormer *Haliotis tuberculata* (L.):
718 Digital shell color analysis. Mar. Biol. 164 (4): 1-13.

719 Martin S, Richier S, Pedrotti ML, Dupont S, Castejon C, Gerakis Y, Kerros ME, Oberhansli
720 F, Teyssie JL, Jeffree R, Gattuso JP (2011) Early development and molecular plasticity
721 in the Mediterranean sea urchin *Paracentrotus lividus* exposed to CO_2-driven
722 acidification. J Exp Biol 214:1357–1368. doi: 10.1242/jeb.051169

723 McClintock JB, Angus RA, Mcdonald MR, Amsler CD, Catledge SA, Vohra YK (2009)
724 Rapid dissolution of shells of weakly calcified Antarctic benthic macroorganisms
725 indicates high vulnerability to ocean acidification. Antarct Sci 21:449–456. doi:
726 10.1017/S0954102009990198

727 McNeill, A. R. 1968. Animal Mechanics; Sidgwick and Jackson, London, United Kingdom.

728 Mehrbach C, Culberson CH, Hawley JE, Pytkowicx RM (1973) Measurement of the apparent
729 dissociation constants of carbonic acid in seawater at atmospheric pressure. Limnol
730 Oceanogr 18:897–907. doi: 10.4319/lo.1973.18.6.0897

731 Melzner F, Gutowska MA, Langenbuch M, Dupont S, Lucassen M, Thorndyke MC, Bleich
732 M, Portner HO (2009) Physiological basis for high CO_2 tolerance in marine ectothermic
733 animals: pre-adaptation through lifestyle and ontogeny? Biogeosciences 6:2313–2331.

734 Melzner F, Stange P, Trübenbach K, Thomsen J, Casties I, Panknin U, Gorb SN, Gutowska
735 MA (2011) Food supply and seawater pCO_2 impact calcification and internal shell

736 dissolution in the blue mussel *Mytilus edulis*. PLOS ONE. doi:
737 10.1371/journal.pone.0024223.

738 Mercer JP, Mai KS, Donlon J (1993) Comparative studies on the nutrition of 2 species of
739 abalone, *Haliotis tuberculata Linnaeus* and *Haliotis discus hannai Ino* . 1. Effects of
740 algal diets on growth and biochemical composition. Invertebr Reprod Dev 23: 75-88.

741 Michaelidis B, Ouzounis C, Paleras A, Pörtner H-O (2005) Effects of long-term moderate
742 hypercapnia on acid–base balance and growth rate in marine mussels *Mytilus*
743 *galloprovincialis*. Mar Ecol Prog Ser 293:109–118.

744 Morash AJ, Alter K (2015) Effects of environmental and farm stress on abalone physiology:
745 perspectives for abalone aquaculture in the face of global climate change. Rev Aquacult
746 7:1–27. doi: 10.1111/raq.12097

747 Morse JW, Arvidson RS, Luttge A (2007) Calcium carbonate formation and dissolution :
748 Chemical Reviews, 107: 342–381, doi: 10.1021/cr050358j.

749 Nicolas JL, Basuyaux O, Mazurié J, Thébault A (2002) *Vibrio carchariae*, a pathogen of the
750 abalone *Haliotis tuberculata*. Dis Aquat Organ 50:35–43.

751 Noisette F, Comtet T, Legrand E, Bordeyne F, Davoult D, Martin S (2014) Does
752 encapsulation protect embryos from the effects of ocean acidification? The example of
753 *Crepidula fornicata*. PLOS ONE. doi: 10.1371/journal.pone.0093021

754 Onitsuka T, Takami H, Muraoka D, Matsumoto Y, Nakatsubo A, Kimura R, Ono T, Nojiri Y
755 (2018). Effects of ocean acidification with pCO_2 diurnal fluctuations on survival and
756 larval shell formation of Ezo abalone, *Haliotis discus hannai*. Mar . Environ. Res. 134,
757 28-36. https://doi.org/10.1016/j.marenvres.2017.12.015²

758 Orr JC, Fabry VJ, Aumont O, Bopp L, Doney SC, Feely RA, Gnanadesikan A, Gruber N,
759 Ishida A, Joos F, Key RM, Lindsay K, Maier-Reimer E, Matear R, Monfray P, Mouchet
760 A, Najjar RG, Plattner G-K, Rodgers KB, Sabine CL, Sarmiento JL, Schlitzer R, Slater
761 RD, Totterdell IJ, Weirig M-F, Yamanaka Y, Yool A (2005) Anthropogenic ocean
762 acidification over the twenty-first century and its impact on calcifying organisms.
763 Nature 437:681–686. doi: 10.1038/nature04095

764 Parker L, Ross P, O'Connor W, Pörtner H, Scanes E, Wright J (2013) Predicting the response
765 of molluscs to the impact of ocean acidification. Biology 2:651–692. doi:
766 10.3390/biology2020651

767 Pierrot DE, Lewis E, Wallace D W R (2006) MS Excel program developed for CO2 system
768 calculations. ORNL/CDIAC-105a. Carbon Dioxide Information Analysis Center. Oak
769 Ridge National Laroratory, US Department of Energy, Oak Ridge, Tennessee.

770 Przeslawski R, Byrne M, Mellin C (2015) A review and meta-analysis of the effects of
771 multiple abiotic stressors on marine embryos and larvae. Glob Change Biol 21:2122–
772 2140. doi: 10.1111/gcb.12833

773 Qui-Minet ZN, Delaunay C, Grall J, Six C, Cariou T, Bohner O, Legrand E, Davoult D,
774 Martin S (2018) The role of local environmental changes on maerl and its associated
775 non-calcareous epiphytic flora in the Bay of Brest. Estuar Coast Shelf Sci 208:140–152.
776 doi: 10.1016/j.ecss.2018.04.032

777 R Core Team (2015) R Core Team: A language and environment for statistical computing.
778 Vienna, Austria

779 Riebesell U, Fabry VJ, Hansson L, Gattuso JP (2010) Guide to best practices for ocean
780 acidification research and data reporting, Publications Office of the European Union.

781 Ross PM, Parker L, O'Connor WA, Bailey EA (2011) The impact of ocean acidification on
782 reproduction, early development and settlement of marine organisms. Water 3:1005–
783 1030. doi: 10.3390/w3041005

784 Shepherd SA (1973) Studies on southern Australian abalone (genus *Haliotis*). I. Ecology of
785 five sympatric species. Aust. J. Mar. Freshwat. Res. 24, 217-257.

786 Talmage SC, Gobler CJ (2010) Effects of past, present, and future ocean carbon dioxide
787 concentrations on the growth and survival of larval shellfish. PNAS 107:17246–17251.
788 doi: 10.1073/pnas.0913804107

789 Thomsen J, Gutowska MA, Saphörster J, Heinemann A, Trübenbach K, Fietzke K,
790 Hiebenthal C, Eisenhauer A, Körtzinger A, Wahl M, Melzner F (2010) Calcifying
791 invertebrates succeed in a naturally CO2-rich coastal habitat but are threatened by high
792 levels of future acidification. Biogeosciences 7:3879–3891. doi.org/10.5194/bg-7-3879-
793 2010

794 Thomsen J, Melzner F (2010) Moderate seawater acidification does not elicit long-term
795 metabolic depression in the blue mussel *Mytilus edulis*. Mar Biol 157:2667–2676. doi:
796 10.1007/s00227-010-1527-0

797 Thomsen J, Haynert K, Wegner KM, Melzner F (2015) Impact of seawater carbonate
798 chemistry on the calcification of marine bivalves. Biogeosciences 12:4209–4220. doi:
799 10.5194/bg-12-4209-2015

800 Travers M-A, Basuyaux O, Le Goic N, Huchette S, Nicolas J-L, Koken M, Paillard C (2009)
801 Influence of temperature and spawning effort on *Haliotis tuberculata* mortalities caused
802 by *Vibrio harveyi*: an example of emerging vibriosis linked to global warming. Glob
803 Change Biol 15:1365–1376. doi: 10.1111/j.1365-2486.2008.01764.x

804 Vogel S. 2003. Comparative Biomechanics. Princeton University Press, Princeton, USA.

805 Waldbusser GG, Steenson RA, Green MA (2011) Oyster shell dissolution rates in estuarine
806 waters: effects of pH and shell legacy. J Shellfish Res 30:659–670.

807 Weiss IM, Lüke F, Eichner N, Guth C, Clausen-Schaumann H (2013) On the function of
808 chitin synthase extracellular domains in biomineralization. J Struct Biol 183:216–225.
809 doi: 10.1016/j.jsb.2013.04.011

810 Welladsen HM, Southgate PC, Heimann K (2010) The effects of exposure to near-future
811 levels of ocean acidification on shell characteristics of *Pinctada fucata* (Bivalvia:
812 Pteriidae). Molluscan Res 30:125–130.

813 Wessel N, Martin S, Badou A, Dubois P, Huchette S, Julia V, Nunes F, Harney E, Paillard C,
814 Auzoux-Bordenave S (2018) Effect of CO_2–induced ocean acidification on the early
815 development and shell mineralization of the European abalone *Haliotis tuberculata*. J
816 Exp Mar Biol Ecol 508:52–63.

817 Widdicombe S, Spicer JI (2008) Predicting the impact of ocean acidification on benthic
818 biodiversity: What can animal physiology tell us? J Exp Mar Biol Ecol 366:187–197.
819 doi: 10.1016/j.jembe.2008.07.024

820 Wittmann AC, Pörtner H-O (2013) Sensitivities of extant animal taxa to ocean acidification.
821 Nat Clim Change 3: 995-1001. doi: 10.1038/NCLIMATE1982

822 Zippay ML, Hofmann GE (2010) Effect of pH on gene expression and thermal tolerance of
823 early life history stages of red abalone (*Haliotis rufescens*). J Shellfish Res 29:429–439.

824

Table 1 Parameters of seawater carbonate chemistry during the experiment (means ± SD). pH on the total scale (pH_T), temperature (°C), salinity and total alkalinity ($\mu Eq.kg^{-1}$) were used to calculate CO_2 partial pressure (pCO_2; µatm), Dissolved Inorganic Carbon (DIC; µmol. kg^{-1}), HCO_3^-, CO_3^{2-}, aragonite saturation state ($\Omega_{aragonite}$) and calcite saturation state ($\Omega_{calcite}$) by using the CO2SYS program. pH_T and temperature are the average values recorded almost daily throughout the experiment (n = 76 per pH treatment). Salinity was measured twice a week (mean 35.3 ± 1.3, n = 26) and total alkalinity was measured every two weeks throughout the experiment (n = 8 per pH treatment).

Nominal pH	pH_T	Temperature (°C)	TA ($\mu Eq.\ kg^{-1}$)	pCO_2 (µatm)	DIC ($\mu mol.kg^{-1}$)	HCO_3^- ($\mu mol.kg^{-1}$)	CO_3^{2-} ($\mu mol.kg^{-1}$)	$\Omega_{aragonite}$	$\Omega_{calcite}$
8.1	8.11 ± 0.04	12.4 ± 1.8	2305 ± 28	335 ± 33	2070 ± 22	1890 ± 35	167 ± 14	2.53 ± 0.22	3.96 ± 0.34
7.8	7.81 ± 0.05	12.1 ± 1.7	2312 ± 30	750 ± 18	2209 ± 18	2088 ± 24	90 ± 10	1.37 ± 0.15	2.14 ± 0.23
7.7	7.71 ± 0.04	12.3 ± 1.7	2308 ± 37	958 ± 108	2237 ± 17	2124 ± 20	74 ± 8	1.12 ± 0.13	1.75 ± 0.2
7.6	7.60 ± 0.05	12.1 ± 1.8	2309 ± 34	1259 ± 140	2274 ± 16	2164 ± 17	58 ± 7	0.88 ± 0.1	1.38 ± 0.16

Supplementary file S1